Smart Structures and Systems, *Vol. 34, No. 2 (2024) 87-96*
https://doi.org/10.12989/sss.2024.34.2.087

Design and fabrication of cost effective semi-active vehicular suspension system and testing on full scale quarter car suspension rig

N.P. Puneet [1a], Radhe Shyam Tak Saini [2b] and Hemantha Kumar*[2]

[1] *Department of Automobile Engineering, Dayananda Sagar College of Engineering, Bengaluru, 560111, India*
[2] *Department of Mechanical Engineering, National Institute of Technology Karnataka, Surathkal, Mangaluru, 575025, India*

(*Received November 24, 2023, Revised September 20, 2024, Accepted September 24, 2024*)

Abstract. Smart materials, such as magnetorheological (MR) fluid, have received considerable research attention in recent years due to their unique capabilities. MR fluid, which possesses a magnetic field controllable viscosity, has been extensively studied for vehicular applications with the aim of synthesizing optimal MR fluids, designing optimal MR dampers, and developing control strategies. However, a comprehensive study that primarily focuses on developing a cost-effective semi-active suspension system for a commercial vehicle in a developing nation is still lacking. This study addresses this gap by synthesizing an in-house MR fluid and studying its rheological properties. Subsequently, a novel single-sensor-based controller is developed and closed-loop simulations are conducted on a quarter-car semi-active model. Finally, the overall semi-active quarter-car suspension system is experimentally tested using a suspension test rig. The performance of the proposed system in terms of ride comfort and road holding is evaluated and is compared with simple control strategies. The dynamic range of the developed semi-active MR damper is found to be around 2.3, indicating a significant MR effect. The results suggest an intermediate response using the proposed acceleration-driven controller (ADV) at lower frequencies and similar performance to that of the skyhook controller at higher frequencies. The cost-effective methodology proposed in this study is effective and can be adapted for other semi-active engineering applications.

Keywords: magneto-rheological fluid; MR damper; quarter car testing; rheology; single sensor system

1. Introduction

Smart materials, particularly magneto-rheological (MR) fluids, are becoming increasingly popular due to their superior characteristics, such as increased strength, flexibility, and responsiveness to external stimuli (Rabinow 1948). MR fluid is a semi-active material that responds to magnetic fields. The ability of MR fluid to adaptively adjust its properties makes it ideal for use in various engineering applications such as clutches, brakes, beams, dampers and other engineering applications. (Rabinow 1948, Acharya *et al*. 2021, Allien *et al*. 2020, Desai *et al*. 2019, Kargar *et al*. 2021). Another interesting application of MR fluids includes their usage in control and vibration suppression of structures by embedding these fluids in the core of sandwich plates (Amir *et al*. 2020a, b, Karger *et al*. 2021).

MR fluid is a suspension of ferrous particles in a base oil with additives that enhance redispersibility and sedimentation stability. Various studies have been performed studying rheological performances of commercial and in-house synthesized MR fluids (Ghaffari *et al*. 2015, Muhammad *et al*. 2006, Jolly *et al*. 1999, Vicente 2013). The challenge is to identify additives that improve sedimentation stability without affecting the rheological performance. Additives that are often used are guar gum, bentonite clay, oleic acid, and aluminium distearate (Acharya *et al*. 2019, Kumbhar *et al*. 2015, Wahid *et al*. 2016). Ferrous particles like carbonyl iron particles and electrolytic iron are also often used (Kumbhar *et al*. 2015, Wahid *et al*. 2016, Puneet *et al*. 2022). The proportions of these constituents greatly affect the rheological performance, allowing customization for specific engineering applications.

One such application that is designed to absorb and damp shock impulses is an MR damper. MR dampers have been the research of interest widely in vehicle and structural applications (Zhang and Agrawal 2015, Maiti *et al*. 2006, Batterbee and Sims 2005). The potential benefits of using semi-active MR dampers in vehicle suspension systems have been reported in various publications. However, the application of semi-active MR dampers has been mostly limited to high-end vehicles, such as the Audi A3 (Audi magnetic ride suspension technology) (Audi Magnetic Ride 2023), Cadillac ATS (Cadillac magnetic ride technology) (Cadillac Magnetic Ride 2023), and Ferrari GTC4Lusso (MagneRide SCM-E suspension) (Ferrari Magneride SCM-E Suspension 2023). More recently, various studies have been conducted to explore the feasibility of this technology in commercial vehicles, both through simulation and experimentation. For example, Desai *et al*. (2019) designed and experimentally characterized a twin-tube MR damper for a passenger van. Jamadar *et al*. (2021) developed a mathematical model for MR damper based on equivalent

*Corresponding author, Ph.D., Professor,
E-mail: hemantha@nitk.edu.in
[a] Ph.D., Assistant Professor
[b] Ph.D., Research Fellow

ISSN: 1738-1584 (Print), 1738-1991 (Online)

damping and showed its efficacy in reducing computational time during real-time control simulations. Babawuro *et al*. (2020) compared active quarter-car suspension against passive suspension systems and employed linear matrix inequality and linear quadratic regulator controllers. Akutain *et al*. (2007) performed a comparative analysis using vertical acceleration data with a modified hybrid semi-active control utilizing skyhook and groundhook concepts. Floreán-Aquino *et al*. (2021) tested a commercial MR damper using skyhook control and compared it with other control schemes. Savaresi *et al*. (2010) proposed a single sensor-based control strategy to reduce cost and increase reliability of a semi-active vehicular suspension system.

The design of semi-active vehicular suspension systems involves the integration of several components, including MR fluid, a damper with an electromagnetic valve, and a control system. Balancing performance with cost poses a significant challenge in this design problem. While many studies have focused on individual aspects related to the optimal design of MR fluid constituents, dampers, and control systems, there is currently no comprehensive study addressing all these elements with the overall objective of cost-effectiveness, to the best of the author's knowledge. The following observations can be made based on the literature studies:

1. MR dampers are only available in high-end vehicles, owing to their high design costs, control sensor and logic implementations, and intellectual patent rights.
2. Most studies on semi-active MR dampers have concentrated on individual areas, such as optimal damper design, determining optimal fluid constituents, and optimal controller design. Furthermore, experimental studies on the real-time implementation of semi-active dampers are limited when compared to analytical and simulation studies.
3. Ride comfort and road-holding performance indices are commonly used to assess control logic performance. Although ride comfort is subjective, both indices are measured in terms of the acceleration values of the sprung and unsprung masses, respectively. Thus, several parameters, including damper geometric dimensions, MR fluid properties, suspension geometry, control logic, and its tunable parameters, affect the performance indices. Optimal damper design for a particular application considering such a large number of parameters adds to the cost of the damper.

Based on the above observations, this study aims to develop a methodology to design a semi-active damper for a commercial four-wheeler vehicle. The cost-effectiveness of the proposed semi-active suspension system is observed in developing an in-house MR fluid (optimally developed for vehicular applications in our previous works (Acharya *et al*. 2019), modifying an already existing passive damper into a semi-active one, reduction of the number of sensors and developing a novel control strategy.

The rest of the paper is organized as follows. The overall methodology of design procedure is detailed in section 2. The rheology of the in-house prepared MR fluid along with the characterization results are provided in section 3. Section 4 and 5 discusses about the retro-fit development and characterization of MR damper respectively. Our novel approach to developing an ADV controller is detailed in section 6. The developed strategy is evaluated for performance both via mathematical modeling in section 7 and experimental studies in section 8. The results are discussed in section 9, followed by conclusions in section 10.

2. Methodology

The primary objective of this study is to design a cost-effective semi-active suspension system. The study presents a detailed methodology starting from the preparation of MR fluid to its usage in a quarter car test assembly. The process of achieving this objective is outlined in this section. Firstly, the MR fluid is prepared in the laboratory using an optimal fraction of constituents. The study of the rheological characterization of the MR fluid for different currents and dynamic conditions are also included. Secondly, an MR damper is designed for a specific four-wheeler vehicle, and its characteristics are studied for various harmonic inputs in a dynamic testing machine. Thirdly, a novel single-sensor-based control logic is developed, and simulation studies are conducted. Lastly, the designed damper is implemented in the McPherson suspension system of a typical commercial vehicle, and the experimental results obtained from a quarter car test setup are compared to simulations. Additionally, the obtained results are compared to various control logics from previous studies.

3. Rheology of in-house MR fluid

Initially, MR fluid is developed using carbonyl iron as ferrous particles, poly alpha olefin as the carrier fluid, and aluminium distearate and bentonite clay as additives. The addition of aluminium distearate enhances the redispersibility of ferrous particles in the MR fluid, while bentonite clay improves its stability by preventing the settling of ferrous particles (Acharya *et al*. 2019). To prepare the MR fluid, the additives are added to the carrier fluid in stages and stirred for 4 hours to ensure a uniform distribution. Carbonyl iron particles are then added to the mixture and stirred for 12 hours, resulting in an MR fluid consisting of 78% carbonyl iron particles and 20% base oil in terms of volume fraction. Both additives are added in equal amounts, constituting a total of 5% of base oil. The rheological properties of the synthesized MR fluid are characterized using a Rheometer. This allows for the study of the MR fluid's rheology with varying magnetic fields for different current inputs. The measurements of shear stress and viscosity for a given shear rate are included in the characterization testing. The experimental setup for rheology testing is illustrated in Fig. 1.

The rheology tests were performed under two conditions: varying shear rate with constant currents and constant shear rate with varying current. During testing,

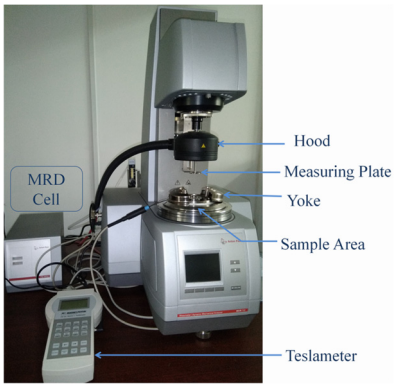

Fig. 1 Rheometer (Make: Anton Paar Pvt Ltd.)

changes in the magnetic field intensity were induced by varying the current. The Rheometer was set up with a shear gap of 0.5 mm between two parallel plates. Fig. 2(a) displays the variations in shear stress with varying shear rate and different currents. The shear rate was adjusted between 1 and 600 s^{-1}. The rheological characterization was conducted with four different current inputs: off-state (0 A), 1 A, 2 A, and 3 A. The recorded shear stress of the MR fluid displayed a significant increase in magnitude as the current input increased.

The MR fluid demonstrates linear shear stress behavior at off-state that is reminiscent of a Newtonian fluid. However, the non-Newtonian nature of the MR fluid is prominently observed when a magnetic field is applied. At a shear rate of 600 s^{-1} and 3A current input, the maximum shear stress increases significantly from 163 Pa to 29,505 Pa as seen in Fig. 2(a). As illustrated in Fig. 2(b), the viscosity of the MR fluid decreases as the shear rate increases. The behavior is consistent for all applied currents, however, apparent viscosity increases with an increase in current. At 600 s^{-1} shear rate, the viscosity of MR fluid in off-state condition is 271.29 mPa.s, which increases to 49,175 mPa.s at a magnetic field corresponding to 3A current.

A set of experiments were also conducted to understand the shear stress and the viscosity variation with current sweep at constant shear rate. Bingham fluid model was used to determine the yield stress and the apparent viscosity. The current input is varied linearly from 0.01A to 5A and the resulting response is depicted in Fig. 3.

The shear stress increased from 245 Pa to 37,613 Pa and the viscosity increased from 819 mPa.s to 125,450 mPa.s with the current sweep. From the rheological characterization results, it is evident that the MR fluid responded favorably to the external magnetic field. Even though the current sweep was linear, the shear stress and viscosity variation have deviated from linearity after a certain point, as shown in Fig. 3. This can be attributed to the saturation limit of magnetic field application on ferrous particles (Acharya *et al*. 2019).

4. Development of MR damper

Fig. 4 illustrates the primary components of the MR damper, which include the cylinder, piston rod, piston with electromagnetic coil, and MR fluid. Together, these components form an electromagnetic circuit, with the cylinder, MR fluid in the shear gap, and the piston serving

(a) Shear stress variation (b) Viscosity variation

Fig. 2 Shear and viscosity variation with varying shear rate

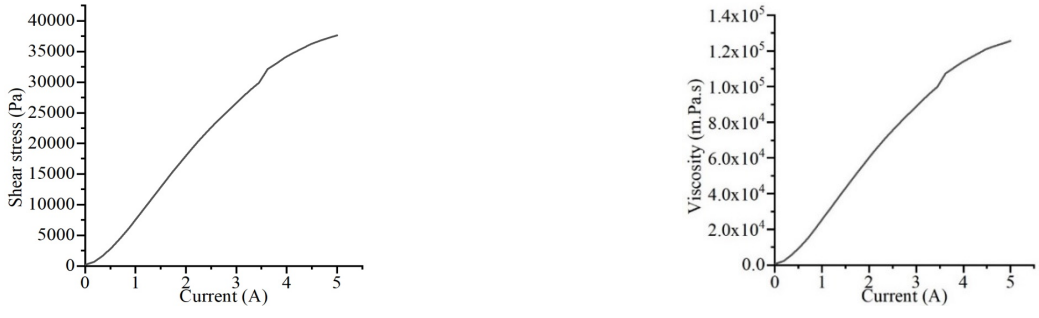

(a) Shear stress variation (b) Viscosity variation

Fig. 3 Shear and viscosity variation with current sweep

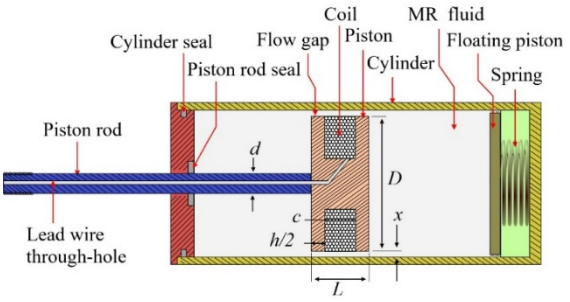

Fig. 4 Schematic diagram of shear mode MR damper

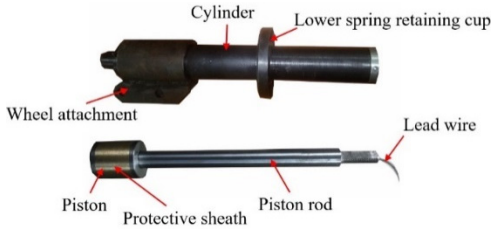

Fig. 5 Fabricated piston and the damper

as the circuit's three key elements. The terminals of the electromagnetic coil are pulled through the piston rod to apply current inputs. The MR damper operates in a shear mode, wherein the piston's relative motion with the cylinder inner surface drives the MR fluid from one chamber to the other. Any change in the current inputs alters the applied magnetic field in the fluid gap, thereby manipulating the rheological properties of the MR fluid and ultimately varying the damping force of the damper.

Achieving optimal design of the MR damper requires solving a multi-physics problem that involves magnetostatic and computational fluid dynamic analysis. However, to simplify the non-Newtonian fluid mechanics, a quasi-static behavior is assumed, resulting in simpler equations that relate to pressure difference (subsequently, the damping force) and piston geometric variables (Yang *et al*. 2002, Phillips 1969, Gavin *et al*. 1996). On the other hand, nonlinear magnetostatic analysis can be simplified by using lumped parameter equivalent magnetic circuit models (Gavin *et al*. 2001, Saini *et al*. 2019, Nguyen and Choi 2009).

In this study, a cost-effective methodology is developed for the design of the damper by retrofitting an optimally designed electromagnetic valve inside the existing damper geometry, converting it into a semi-active damper. A volume-constrained optimization problem is formulated to determine the highest magnetic field in the flow gap region without exposing any part of electromagnetic circuit to saturation. The procedure for volume-constrained optimal design is provided elsewhere (Acharya *et al*. 2019, Saini *et al*. 2019), and the optimal dimensions of the damper, rounded off, shown in Table 1. All materials used in the electromagnetic circuit, except for the cylinder, are fabricated with American Iron and Steel Institute 1018 (AISI 1018) steel.

American wire gauge 25 (AWG 25) copper wire is wound around the piston with 300 turns. The developed MR damper is depicted in Fig. 5. Also, a spring accumulator is placed at the bottom position of the damper to accommodate for the volume difference arising due to the movement of the piston rod in the cylinder.

Table 1 Dimensions of piston and electromagnetic valve

Piston specification	Dimension (mm)
Piston head diameter (D)	36
Piston rod diameter (d)	20
Pole length (h)	10
Total piston head length (L)	50
Annular flow gap (x)	1

5. Characterization of MR damper

In order to comprehend the dynamic response of the MR damper, a characterization analysis of the assembled damper is conducted with various harmonic inputs on a dynamic testing machine. Fig. 6(a) depicts a schematic diagram of the damper testing machine (DTM). For any selected input, the controller provides a signal to the servo valves, which controls the motion of the actuator backed by hydraulic power supply. The actuating signal excites the damper under study, and a load cell measures the damping force exerted by the device. In addition, a DC power supply is used to provide current input to the electromagnetic coil in the damper in order to estimate the damping effect of MR fluid under the influence of various magnetic fields. The acquired sensory data is measured by a data acquisition system and recorded for subsequent analysis. The experimental test setup of the dynamic testing machine attached with an MR damper is presented in Fig. 6(b).

The MR damper is subjected to harmonic excitations with varying amplitudes and frequencies. Along with these, the performance of MR damper is observed for different current excitations varying from 0 A (off-state) to 1 A in steps of 0.25 A. The current input to the damper is provided by direct current (DC) power supply. The characterization of MR damper is performed for various sinusoidal input displacements. However, for the sake of brevity, results related to 10 mm amplitude and 2 Hz frequency for varying current inputs are provided, as seen in Fig. 7.

Based on the results of the characterization of the MR damper, it is evident that the total damping force generated in the off-state condition is approximately 411 N (rebound) and -191 N (compressive). Similarly, when a 1A current input is applied to the piston of the MR damper, the damping forces recorded are 808 N (rebound) and -540 N (compressive). As can be inferred from the characterization data, the compression and rebound forces are asymmetrical, which could be attributed to the usage of a spring accumulator within the damper. Although the spring accumulator prevented the problem of lateral shift, the magnitude of the spring force could be a reason behind the asymmetry between the compression and rebound force. The testing of the MR damper at other current conditions also revealed a significant difference in the damping forces

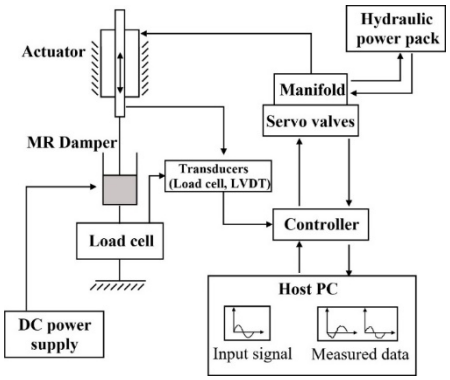

(a) Dynamic testing machine schematic

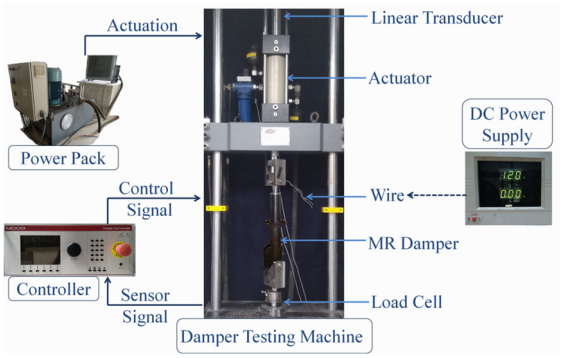

(a) Dynamic testing machine schematic

Fig. 6 Schematic and experimental setup of dynamic testing machine installed with MR damper (in the figure LVDT is abbreviated form of Linear variable differential transformer)

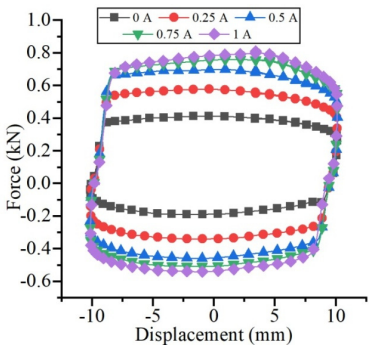

(a) Force-displacement curves

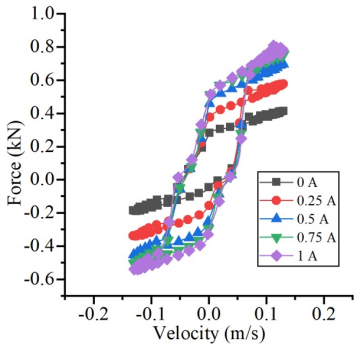

(b) Force-velocity curves

Fig. 7 Damper characterization curves at 10 mm amplitude, 2 Hz frequency and at varying currents

(refer to Fig. 7). This design yielded a dynamic range of 2.3, which is comparable to other dampers intended for vehicular applications (Devikiran *et al*. 2022, Yu *et al*. 2006). Also, a slight horizontal shift between the lower and upper characteristic curve can be observed. As compared to previous studies, this shift is minimal, thus suggesting that the use of floating piston resulted in reduction of cavitation effects in the damper.

6. Controller

Numerous control approaches have been developed in previous studies for semi-active vehicle suspension, which can generally be categorized as linear, nonlinear, or robust controllers. Linear controllers, such as skyhook and groundhook, are considered the simplest to implement. However, the cost of hardware to implement the control logic and the required sensors for feedback can be a significant factor. The aforementioned controllers necessitate at least two sensors to obtain feedback data. Thus, in this study, a low-cost, single-sensor-based controller is designed, and the control logic is executed using inexpensive sensors and microcontroller. The efficacy of the proposed controller is evaluated and compared with that of the widely used skyhook controller, which is known for its simplicity and effectiveness in improving ride comfort.

6.1 Acceleration driven velocity (ADV) control

Recent studies have demonstrated that the longitudinal acceleration of the car body can be used to estimate road profile and surface condition. It was shown that there exists a correlation between the mean amplitude value of body acceleration and the road surface roughness (Praznowski *et al*. 2020, Nguyen *et al*. 2019, Zhao *et al*. 2019). Based on this finding, the current supplied to the damper is modulated according to the root mean square (RMS) values of sprung mass accelerations. As only one sensor is required to measure the body acceleration, this approach can effectively reduce the overall cost of the controller.

The control strategy involves setting the damping constant to a low value when the RMS value of sprung mass acceleration exceeds a specified threshold, while regulating it to a maximum using Eq. (1) when it falls below the threshold. This approach provides a simple and cost-effective method of controlling the semi-active suspension system (Savaresi *et al*. 2010).

$$c_{in} = \begin{cases} c_{min} & if \quad \ddot{z}_{RMS} \geq a_{threshold} \\ c_{max} & \text{otherwise} \end{cases} \tag{1}$$

Here, c_{min} is the minimum damping constant equivalent to zero current, c_{max} is the maximum damping constant equivalent to high current, $\ddot{z}_{RMS}$ is the RMS

acceleration of sprung mass acceleration evaluated over a moving window, and $a_{threshold}$ is the acceleration threshold which can be user controlled.

6.2 Skyhook control

This is a simple on/off strategy which switches between high and low damping coefficients in order to achieve the required levels of comfort or road holding (Akutain *et al*. 2007). The control law is given by the Eq. (2)

$$c_{in} = \begin{cases} c_{min} & if \quad \dot{z}\dot{z}_{def} \leq 0 \\ c_{max} & if \quad \dot{z}\dot{z}_{def} > 0 \end{cases} \tag{2}$$

Here, $\dot{z}$ is the sprung mass velocity and $\dot{z}_{def}$ is the deflection velocity. From an implementation point of view, it requires two measurements and thus two sensors for each wheel.

7. Mathematical modeling

7.1 Quarter car model

The quarter car model is a simplified representation of a vehicle's suspension system, used for analyzing and evaluating the performance of the system. It consists of a sprung mass, representing the vehicle body, and an unsprung mass, representing the wheels and suspension components. The two masses are connected by a spring and a damper, which represent the suspension system. The suspension elements, namely the spring and damper, are designed to reduce the effects of these disturbances on the vehicle body, and provide a smoother ride for the occupants. A two degree of freedom quarter car model as shown in Fig. 8 is used in this study.

The mathematical model of the quarter car model is defined by following Eqs. (3)-(4) (Jamadar *et al*. 2021)

$$m_1\ddot{z}(t) + k_1(z - z_t) + c_1(\dot{z} - \dot{z}_t) = 0 \tag{3}$$

$$\begin{aligned} &m_2\ddot{z}_t(t) - k_1(z - z_t) - c_1(\dot{z} - \dot{z}_t) \\ &+k_2(z_t - z_r) + c_2(\dot{z}_t - \dot{z}_r) = 0 \end{aligned} \tag{4}$$

Here, m_1 is the mass of sprung mass, m_2 is the mass of unsprung mass, k_1 is the suspension spring constant, c_1 is the suspension damping constant which is being modulated by the controller, k_2 is the tire stiffness, c_2 is the tire damping, z is the sprung mass deflection, z_t is the unsprung mass deflection and z_r is the vertical deflection of road. The parameters used in this study are given in Table 2.

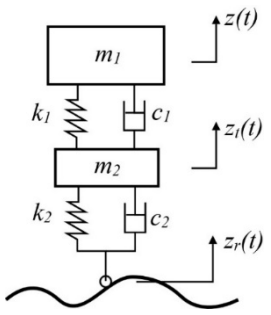

Fig. 8 Quarter car model

Table 2 Quarter car simulation parameters

Parameter	Value (units)
m_1	600 (kg)
m_2	75 (kg)
k_1	30000 (N/m)
k_2	300000 (N/m)
c_1	1516 (Ns/m)
c_2	0 (Ns/m)
c_{max}	4000 (Ns/m)
c_{min}	700 (Ns/m)

7.2 Comparison metrics

To compare responses generated by various control algorithms, a method detailed in Savaresi *et al*. (2010) is used. The method is described below.

1. A sinusoidal road input given by Eq. (5) is fed to the quarter car model over a period of 10 cycles.

$$z_r = A\,sin(2\pi ft) \tag{5}$$

   Here, A is the amplitude of the road profile, f is the frequency and t is time in seconds in the range [0, 10/f].
2. The corresponding output displacement plots of sprung mass (z) and relative displacement of tire $(z_{rel} = z_t - z_r)$ are recorded.
3. Power spectral densities of road input (Z_r), sprung mass displacement (Z) and relative tire displacement (Z_{rel}) are evaluated.
4. The corresponding frequency plots for ride comfort and road holding are generated as ratios $Z(f)/Z_r(f)$ and $Z_{rel}(f)/Z_r(f)$ for all road input frequencies, $Z_r(f)$.

This methodology allows to derive Bode like diagrams for nonlinear systems and thus can be used in comparative studies of control algorithms.

8. Experimental testing on quarter car

The developed MR damper has its compatibility in terms of dimension with the suspension system of a definite light motor vehicle. This work used the McPherson suspension system for the damper installment. A schematic of the quarter car suspension test rig is depicted in Fig. 9(a), wherein vertical motion representing road undulations is imparted to the actuation table by an actuator, and the tire of the quarter car structure is placed atop it. The suspension system, consisting of the McPherson strut assembly in this case, is affixed to the wheel unit and the bottom plate of the

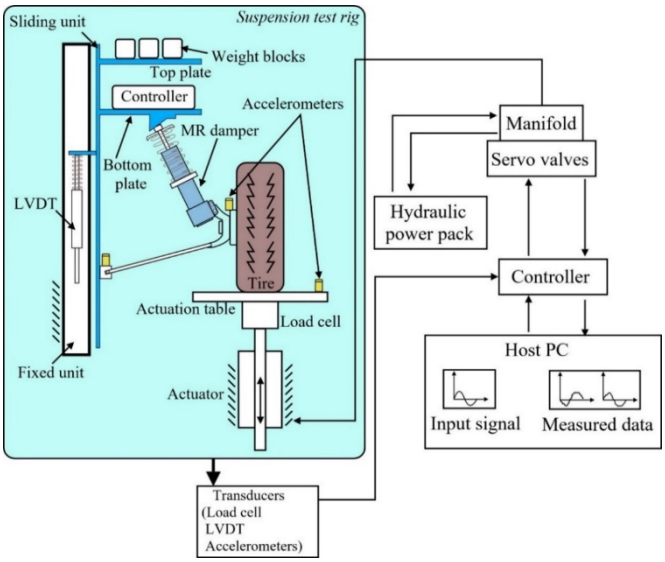

(a) Schematic of quarter car suspension test rig

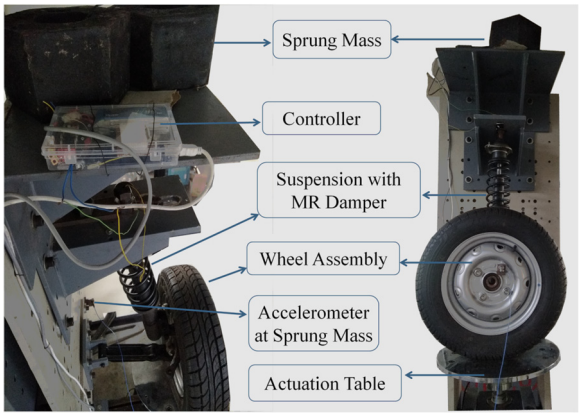

(b) Experimental quarter car suspension test rig

Fig. 9 Schematic and experimental setup of quarter car suspension test rig incorporated with MR damper

sliding unit. The sliding unit, along with the bottom and top plates, controller, and weight blocks, represents the sprung mass, which can be adjusted using weight blocks. The sliding unit is permitted to move in the vertical direction, thereby simulating the vertical displacement of the vehicle. Several sensors, as shown in Fig. 9(a), are positioned on the test rig to measure simulated road displacements, sprung and unsprung mass accelerations, and sprung mass displacement. All sensor signals are acquired by data acquisition systems and recorded for subsequent analysis.

The suspension system is then fitted along with other components required in a quarter car set up. The sprung mass is placed over the suspension system and the sprung mass was set to be 210 kg, which represents the quarter mass of a commercial light motor vehicle. The spring element was the commercially available one that came along with the McPherson system of the vehicle. The resulting quarter car structure, equipped with the MR damper in the McPherson suspension, is illustrated in Fig. 9(b). Due to experimental limitations and to avoid excessive vibrations, experiments have only been carried out in the range of 1 to 7 Hz in the interval of 0.1 Hz and for an amplitude of 10 mm in a sinusoidal profile.

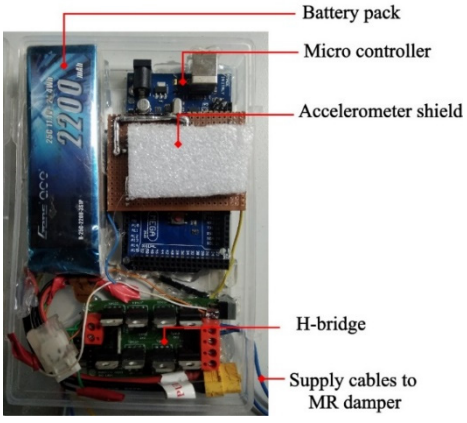

Fig. 10 Developed compact controller

8.1 ADV controller

A compact controller has been developed to supply input current to the damper, as shown in Fig. 10. The controller consists of an Arduino microprocessor, GY61 accelerometer sensor, a 12V DC power supply, and an H-

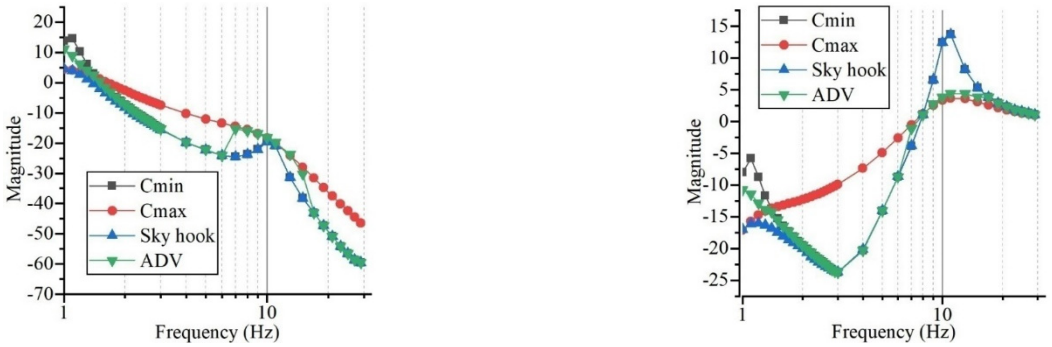

(a) Ride comfort frequency responses (b) Road holding frequency responses

Fig. 11 Nonlinear frequency response curves for ride comfort and road holding

bridge module. Based on the acceleration values of the sprung mass, the input current to the MR damper is regulated on-off, corresponding to (c_{max}, c_{min}) damping constant. For a sampling frequency of 1000 Hz and RMS calculations for a moving window of 500 time steps were considered. Since the moving window is kept constant and to avoid redundant calculations, sum of squares (SS) values of accelerations in the moving window are used instead of RMS values.

The following algorithm, which makes use of previous time step calculations, is used in the microcontroller.

1. Initialize the parameters, *BufferSize* = 500, *counter* = 0, array *AR*[*BufferSize*] = 0, *SS* = 0.
2. Record the acceleration sensor reading in the variable *z*.
3. Calculate the sum of square values, *SS* = *SS*+ *z***z* – *AR[counter]***AR[counter]*
4. Initialize *AR*[*counter*] = *z*.
5. Increment *counter* value.
6. Reinitialize the value of *counter* to 0, if *counter* < *BufferSize* – 1.
7. Regulate damper current based on *SS* values and repeat the process from steps 2 to 6.

9. Results and discussion

Numerical studies were conducted to analyze ride comfort and road holding for a 10 mm displacement, resulting in nonlinear frequency plots. An acceleration threshold of 0.35 m/s^2 was implemented to demonstrate the effectiveness of the control algorithm. The obtained results revealed that for low frequencies ranging between 1-1.4 Hz, stiff damping yielded the optimal filtering performance, whereas soft damping exhibited significant attenuation, ultimately resulting in improved comfort. These findings are supported by the results displayed in Fig. 11(a).

The skyhook controller exhibits superior ride comfort for both higher and lower frequency components. In contrast, the proposed ADV controller exhibits an intermediate response in the low frequency range and a response similar to the skyhook controller in the high frequency range.

Regarding road holding, the frequency plots indicate that for higher frequencies within the 8 – 17 Hz range, soft damping results in poorer road holding, whereas stiff suspension yields better filtering performance. Notably, the skyhook controller performs worse in higher frequency ranges, similar to soft damping as shown in Fig. 11(b). In contrast, the proposed controller performs comparably to the stiff damper and results in improved road holding characteristics. A transition point around 6 Hz can be noticed for the proposed controllers where the ADV controller transitions from the soft damping to hard damping. This switching frequency can be varied by selecting the acceleration threshold. Therefore, the proposed controller provides selective performance in enhancing both ride comfort and road holding.

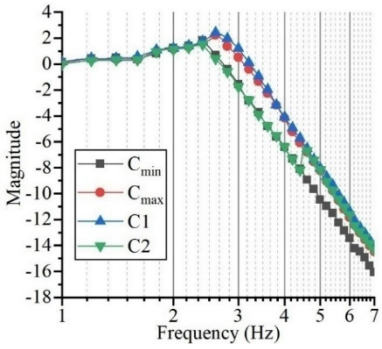

Fig. 12 Experimental nonlinear frequency ride comfort characteristics

Fig. 12 illustrates the experimental results for nonlinear ride comfort at various frequencies. Two separate case studies were conducted, one by setting an acceleration threshold of 0.25 m/s^2 (hereafter referred to as ‘C1’ in subsequent analysis), and the other at 0.35 m/s^2 (hereafter referred to as ‘C2’). Due to the much lower acceleration threshold value of 0.25 m/s^2, the controller ‘C1’ transitions to hard damping after 2.4 Hz. In contrast, the controller ‘C2’ exhibits a transition point at approximately 4.4 Hz, at which point the damping characteristics modulate from soft to hard damping, as shown in Fig. 12. After this frequency, the RMS accelerations of the sprung mass exceed the limit of 0.35 m/s^2, leading to a transition from soft to stiff damping in the suspension system.

Owing to experimental limitations, road holding analysis and responses to random road profiles were not conducted. Nevertheless, the experimental results for ride

Table 3 Cost comparison between commercial and developed one

Component	Cost of commercial one (INR)	Cost of developed one (INR)
MR Damper	83000	39000
Controller	21000	4300
Total	104000	43300

comfort exhibit a similar trend as that of the simulation results, which is evident from Figs. 11(a) and 12.

Lastly, a cost comparison between the damper models available commercially and the one fabricated in this study is performed. Due to non-availability of prices of semi-active dampers of high end vehicles, a comparison with that of commercially available seat suspension dampers is performed. As can be seen in Table 3, a significant cost reduction of more than 50 % can be achieved by using the damper designed in this study.

10. Conclusions

The current study emphasizes the development of a cost-effective semi-active suspension system for a four-wheeler vehicle. In this regard, a comprehensive study starting from the preparation of MR fluid with optimal constituents to experimental testing was conducted. After performing rheological characterization on the optimal MR fluid, a passive damper of a typical commercial vehicle of McPherson type was optimally designed to realize a semi-active damper. Later, the semi-active damper was characterized using various harmonic inputs and was found to have a dynamic range of 2.3, which is on par with those of previous studies. A novel control strategy was proposed which regulates the current supplied to the damper based on the sum of square values of sprung mass acceleration in a moving horizon window. Subsequently, simulation studies were performed on the overall semi-active quarter car model coupling with the proposed controller and the control performances were compared to those of various passive dampers and skyhook controller. Finally, experimental studies were conducted on a suspension test rig using McPherson strut assembly fit with the developed semi-active damper and the ride comfort was evaluated for the proposed controller. It was observed that the experimental results agree well with those of simulation trends. Overall, in this study a cost-effective methodology is proposed which can be similarly applied to develop other semi-active dampers for commercial vehicles in developing nations.

Acknowledgments

This work received the funding support by the Ministry of Human Resource Development and Ministry of Road Transport and Highways, Govt. of India under IMPRINT project titled with "Development of Cost-Effective Magneto-Rheological (MR) Fluid Damper in Two wheelers and Four Wheelers Automobile to Improve Ride Comfort and Stability" [No. IMPRINT/2016/7330].

References

Acharya, S., Saini, R.S.T. and Kumar, H. (2019), "Determination of optimal magnetorheological fluid particle loading and size for shear mode monotube damper", *J. Brazilian. Soc. Mech. Sci. Eng.*, **41**, 1-15. https://doi.org/10.1007/s40430-019-1895-4

Acharya, S., Saini, T.R.S., Sundaram, V. and Kumar, H. (2021), "Selection of optimal composition of MR fluid for a brake designed using MOGA optimization coupled with magnetic FEA analysis", *J. Intell. Mater. Syst. Struct.*, **32**(16), 1831-1854. https://doi.org/10.1177/1045389X20977905

Akutain, X.C., Vinolas, J., Savall, J. and Castro, M. (2007), "Comparing the performance and limitations of semi-active suspensions", *Int. J. Veh. Syst. Model. Test.*, **2**, 296. https://doi.org/10.1504/IJVSMT.2007.016239

Allien, J.V., Kumar, H. and Desai, V. (2020), "Semi-active vibration control of MRF core PMC cantilever sandwich beams: Experimental study", *Proceedings of the Institution of Mechanical Engineers, Part L: Journal of Materials: Design and Applications*, **234**, 574-585. https://doi.org/10.1177/1464420720903078

Amir, S., Arshid, E., Khoddami Maraghi, Z., Loghman, A. and Ghorbanpour Arani, A. (2020a), "Vibration analysis of magnetorheological fluid circular sandwich plates with magnetostrictive facesheets exposed to monotonic magnetic field located on visco-Pasternak substrate", *J. Vib. Control*, **26**(17-18), 1523-1537. https://doi.org/10.1177/1077546319899203

Amir, S., Arshid, E. and Maraghi, Z.K. (2020b), "Free vibration analysis of magneto-rheological smart annular three-layered plates subjected to magnetic field in viscoelastic medium", *Smart Struct. Syst., Int. J.*, **25**(5), 581-592. https://doi.org/10.12989/sss.2020.25.5.581

Audi Magnetic Ride, Accessed 6 April 2023; https://www.audi-technology-portal.de/en/chassis/suspension-control-systems/audi-magnetic-ride_en

Babawuro, A.Y., Tahir, N.M., Muhammed, M. and Sambo, A.U. (2020), "Optimized state feedback control of quarter car active suspension system based on LMI algorithm", *Journal of Physics: Conference Series. IOP Publishing*, **1502**(1), 012019. https://doi.org/10.1088/1742-6596/1502/1/012019

Batterbee, D.C. and Sims, N.D. (2005), "Vibration isolation with smart fluid dampers: a benchmarking study", *Smart Struct. Syst., Int. J.*, **1**(3), 235-256. https://doi.org/10.12989/sss.2005.1.3.235

Cadillac Magnetic Ride, Accessed 6 April 2023; https://www.schepelcadillac.com/cadillac-magnetic-ride-control-portage-in.html

Desai, R.M., Jamadar, M.E.H., Kumar, H., Joladarashi, S. and Raja Sekaran, S.C. (2019), "Design and experimental characterization of a twin-tube MR damper for a passenger van", *J. Brazilian. Soc. Mech. Sci. Eng.*, **41**, 1-21. https://doi.org/10.1007/s40430-019-1833-5

Devikiran, P., Puneet, N.P., Hegale, A. and Kumar, H. (2022), "Design and development of MR damper for two wheeler application and Kwok model parameters tuning for designed damper", *Proceedings of the Institution of Mechanical Engineers, Part D: Journal of Automobile Engineering*, **236**, 1595-1606. https://doi.org/10.1177/09544070211036317

Ferrari Magnaride SCM-E Suspension, Accessed 6 April 2023; https://www.ferrari.com/en-EN/auto/gtc4lussot

Floreán-Aquino, K.H., Arias-Montiel, M., Linares-Flores, J., Mendoza-Larios, J.G. and Cabrera-Amado, A. (2021), "Modern semi-active control schemes for a suspension with MR actuator for vibration attenuation", *Actuators*, **10**(2), 22. https://doi.org/10.3390/act10020022

Gavin, H.P., Hanson, R.D. and Filisko, F.E. (1996), "Electrorheological dampers, part I: analysis and design", *J.*

Appl. Mech., **63**(3), 669-675. https://doi.org/10.1115/1.2823348
Gavin, H., Hoagg, J. and Dobossy, M. (2001), "Optimal Design of Magnetorheological Dampers", *Proc. US-Japan. Work. Smart. Struct. Improv. Seism. Perform. Urban. Reg.*, 225-236.
Ghaffari, A., Hashemabadi, S.H. and Ashtiani, M. (2015), "A review on the simulation and modeling of magnetorheological fluids", *J. Intell. Mater. Syst. Struct.*, **26**, 881-904. https://doi.org/10.1177/1045389X14546650
Jamadar, M.E.H, Desai, R.M., Saini, R.S.T., Kumar, H. and Joladarashi, S. (2021), "Dynamic analysis of a quarter car model with semi-active seat suspension using a novel model for magneto-rheological (MR) damper", *J. Vib. Eng. Technol.*, **9**, 161-176. https://doi.org/10.1007/s42417-020-00218-1
Jolly, M.R., Bender, J.W. and Carlson, J.D. (1999), "Properties and Applications of Commercial Magnetorheological Fluids", *J. Intell. Mater. Syst. Struct.*, **10**, 5-13. https://doi.org/10.1177/1045389X9901000102
Kargar, J., Arani, A.G., Arshid, E. and Rahaghi, M.I. (2021), "Vibration analysis of spherical sandwich panels with MR fluids core and magneto-electro-elastic face sheets resting on orthotropic viscoelastic foundation", *Struct. Eng. Mech., Int. J.*, **78**(5), 557-572. https://doi.org/10.12989/sem.2021.78.5.557
Kumbhar, B.K., Patil, S.R. and Sawant, S.M. (2015), "Synthesis and characterization of magneto-rheological (MR) fluids for MR brake application", *Eng. Sci. Technol. Int. J.*, **18**, 432-438. https://doi.org/10.1016/j.jestch.2015.03.002
Madhavrao, Desai, R., Acharya, S., Jamadar M.E.H., Kumar, H., Joladarashi, S. and Sekaran, S.R. (2020), "Synthesis of magnetorheological fluid and its application in a twin-tube valve mode automotive damper", *Proc. Inst. Mech. Eng. Part. L. J. Mater. Des. Appl.*, **234**(7), 1001-1016. https://doi.org/10.1177/1464420720925497
Maiti, D.K., Shyju, P.P. and Vijayaraju, K. (2006), "Vibration control of mechanical systems using semi-active MR-damper", *Smart Struct. Syst., Int. J.*, **2**(1), 61-80. https://dx.doi.org/10.12989/sss.2006.2.1.061
Muhammad, A., Yao, X. and Deng, Z. (2006), "Review of magnetorheological (MR) fluids and its applications in vibration control", *J. Mar. Sci. Appl.*, **5**, 17-29. https://doi.org/10.1007/s11804-006-0010-2
Nguyen, Q.H. and Choi, S.B. (2009), "Optimal design of a vehicle magnetorheological damper considering the damping force and dynamic range", *Smart Mater. Struct.*, **18**(1), 015013. https://doi.org/10.1088/0964-1726/18/1/015013
Nguyen, T., Lechner, B. and Wong, Y.D. (2019), "Response-based methods to measure road surface irregularity: a state-of-the-art review", *Eur. Transp. Res. Rev.*, **11**, 43. https://doi.org/10.1186/s12544-019-0380-6
Phillips, R.W. (1969), "Engineering applications of fluids with a variable yield stress", Ph.D. Dissertation; University of California, Berkeley, CA, USA.
Prażnowski, K., Mamala, J., Śmieja, M. and Kupina, M. (2020), "Assessment of the road surface condition with longitudinal acceleration signal of the car body", *Sensors*, **20**, 5987. https://doi.org/10.3390/s20215987.
Puneet, N.P., Devikiran, P., Kumar, H. and Gangadharan, K.V. (2022), "Performance evaluation of magneto-rheological damper through characterization testing, modeling and its implementation in quarter car", *J. Vib. Eng. Technol.*, **10**, 967-983. https://doi.org/10.1007/s42417-021-00422-7
Rabinow, J. (1948), "The Magnetic Fluid Clutch", *Trans. Am. Inst. Electr. Eng.*, **67**, 1308-1315. https://doi.org/10.1109/T-AIEE.1948.5059821
Saini, R.S.T., Kumar, H., Chandramohan, S. and Srinivasan, S. (2019), "Design of twin-rod flow mode magneto rheological damper for prosthetic knee application", In: *AIP Conference Proceedings*, **2200**, 020045. https://doi.org/10.1063/1.5141215
Savaresi, S., Poussot-Vassal, C., Spelta, C., Sename, O. and Dugard, L. (2010), *Semi-Active Suspension Control Design for Vehicles*, Elsevier. https://doi.org/10.1016/B978-0-08-096678-6.00023-7
Vicente, J. de. (2013), "Magnetorheology : a review", e-rheo-iba, 1, pp. 1-18.
Wahid, S.A., Ismail, I., Aid, S. and Rahim, M.S.A. (2016), "Magneto-rheological defects and failures: A review", In: *IOP Conference Series*: *Materials Science and Engineering*, **114**(1), 012101. https://doi.org/10.1088/1757-899X/114/1/012101
Yang, G., Spencer, B.F., Carlson, J.D. and Sain, M.K. (2002), "Large-scale MR fluid dampers: Modeling and dynamic performance considerations", *Eng. Struct.*, **24**, 309-323. https://doi.org/10.1016/S0141-0296(01)00097-9
Yu, M., Liao, C.R., Chen, W.M. and Huang, S.L. (2006), "Study on MR semi-active suspension system and its road testing", *J. Intell. Mater. Syst. Struct.*, **17**, 801-806. https://doi.org/10.1177/1045389X06057534
Zhang, J. and Agrawal, A.K. (2015), "An innovative hardware emulated simple passive semi-active controller for vibration control of MR damper", *Smart Struct. Syst., Int. J.*, **15**(3), 831-846. https://dx.doi.org/10.12989/sss.2015.15.3.831
Zhao, B., Nagayama, T. and Xue, K. (2019), "Road profile estimation, and its numerical and experimental validation, by smartphone measurement of the dynamic responses of an ordinary vehicle", *J. Sound. Vib.*, **457**, 92-117. https://doi.org/10.1016/j.jsv.2019.05.015